energies

MDPI

Article

The Temporal and Spatial Characteristics of Wind–Photovoltaic–Hydro Hybrid Power Output Based on a Cloud Model and Copula Function †

Haoling Min [1], Pinkun He [1], Chunlai Li [2], Libin Yang [2] and Feng Xiao [1,*]

[1] School of Water Resources and Hydropower Engineering, North China Electric Power University, Beijing 102206, China; hlmin@ncepu.edu.cn (H.M.); 15861837172@163.com (P.H.)
[2] Economic and Technological Research Institute, State Grid Qinghai Electric Power Company, Xining 810000, China
* Correspondence: xiaofeng@ncepu.edu.cn
† This paper is an extended version of our paper published in 2022 6th International Conference on Power and Energy Engineering Conference, Shanghai, China, 25–27 November 2022; pp. 7–11.

Abstract: In a high proportion of wind–photovoltaic–hydro hybrid power systems, fluctuation and dispersion make it difficult to accurately quantify the output characteristics. Therefore, in this study, a cloud model and copula correlation coefficient matrix were constructed for a hybrid power generation system based on the output data. Multiple backward cloud transformation based on the sampling-with-replacement method was proposed to calculate the improved entropy and hyperentropy to analyze the fluctuation range and dispersion degree quantitatively. A similarity index was proposed to evaluate the similarity between wind power, PV power, and hydropower. A suitable copula function was selected, and the Kendall and Spearman coefficients show the correlation relationships of the hybrid systems. The temporal and spatial characteristics of the hybrid systems were analyzed based on the two models. A typical example in Qinghai proved the effectiveness and applicability of the method. The results show that the correlation between photovoltaic power and hydropower is better and that, in summer, hydropower can be used to adjust the output of renewable energy.

Keywords: cloud model; copula function; hybrid power system; similarity index; correlation coefficient

check for updates

Citation: Min, H.; He, P.; Li, C.; Yang, L.; Xiao, F. The Temporal and Spatial Characteristics of Wind–Photovoltaic–Hydro Hybrid Power Output Based on a Cloud Model and Copula Function. *Energies* **2024**, *17*, 1024. https://doi.org/10.3390/en17051024

Academic Editor: Abdul-Ghani Olabi

Received: 22 January 2024
Revised: 12 February 2024
Accepted: 16 February 2024
Published: 22 February 2024

Copyright: © 2024 by the authors. Licensee MDPI, Basel, Switzerland. This article is an open access article distributed under the terms and conditions of the Creative Commons Attribution (CC BY) license (https://creativecommons.org/licenses/by/4.0/).

1. Introduction

With the rapid development of renewable energy and the goals of energy policies [1], the impact of high-penetration power systems is becoming increasingly obvious [2]. Wind power and photovoltaic power have strong randomness and volatility [3]. Large-scale integration into the power grid will cause the problem of insufficient system flexibility [4], which, in turn, will cause large-scale power abandonment [5]. Given its large scale [6], good regulation performance [7], and clean, environmentally friendly, and high-quality energy [8], hydropower can effectively stabilize the output fluctuations in wind and photovoltaic power [9]. In the current energy context, wind power, photovoltaic power, and hydropower have gained importance due to their abundant resources and low pollution [10]. Constructing a high proportion of clean-energy power systems is an inevitable trend in the development of global power systems [11].

In order to analyze the temporal and spatial characteristics of the wind–photovoltaic–hydro hybrid power output, researchers have carried out a large amount of research from different perspectives [12]. On the one hand, many researchers only pay attention to the simple mathematical model of hybrid stations [13]. For instance, Zhao et al. quantified and evaluated the degree of power generation complementarity of various energy systems within a certain time scale by defining a complementary coefficient [14]. Chen et al. used

the copula function to model and describe the load-matching abilities of multiple renewable energy stations so as to obtain the complementary evaluation of the renewable energy outputs [15]. Tan et al. used the output curve to analyze the complementary characteristics of the wind power–photovoltaic power–hydropower system from the perspective of natural and technical characteristics [16]. These models fail to analyze the inherent correlation characteristics of the complementary system output.

On the other hand, at present, the analysis of output power mostly adopts the method of data mining to establish the mapping relationships between the input variables and output of each power generation system [17]. When extreme conditions occur, this deterministic model cannot accurately reflect the overall output of the system [18]. Due to the randomness and fuzziness of renewable energy output, the output curve cannot strictly reflect the change in output [19], and the actual output value should change within a certain range. The cloud model is an algorithm that combines randomness and fuzziness [20]. It is a cognitive model based on the theory of the probability measure space [21]. The model realizes the problems of bidirectional transformation between the qualitative perspective and quantitative perspective [22]. Therefore, it is of great significance to establish a cloud model to describe the output of multi-energy complementary generation systems [23]. Nowadays, there are few studies that build correlation relationships with cloud models. Wang et al. used the cloud model to analyze the correlation between the indicators and warnings of the transmission line operation status [24]. However, single-cloud models fail to construct high-dimensional models. Copulas are widely used to construct multivariate probabilities [25]. Due to the systematic theories, copulas have advantages in correlations between multiple variables [26]. The copula function is often used to measure the correlations of hybrid complementary systems [27]. Because cloud models can only capture the two-dimensional similarity, three-dimensional copulas are constructed to analyze the correlations of wind power–photovoltaic power–hydropower hybrid systems. In addition, the copula function can be used to effectively construct the mathematical relationship between wind power, photovoltaic power, and hydropower. Therefore, the copula function can not only build the correlation coefficient but also improve the computation efficiency. Lin et al. proposed the multivariate Gaussian kernel copula to describe the correlation of wind speeds among multiple wind farms [28]. It is difficult to obtain the exact correlation under different operating conditions with a single copula function.

Based on the idea of the cloud model and copula function, this paper establishes a correlation model to analyze the temporal and spatial characteristics of the wind–photovoltaic–hydro hybrid power output based on the cloud model and copula function.

2. Research Methodology

2.1. Basic Output Cloud

The cloud model combines the randomness and fuzziness of events through three characteristic indexes (expectation E_x, entropy E_n, and hyperentropy H_e) to form the transformation and mapping between qualitative analysis and quantitative analysis [29]. In this section, the basic structure of cloud theory is given, along with a description of the uncertainty in hybrid systems.

U is a common set of variables x.The set can be described as $U = \{x\}$, and U is a quantitative domain called the domain of discourse. Assume that C is a random qualitative concept on the quantitative domain U. If the quantitative data set $x \in U$ is a random realization of the qualitative concept $\mu(x) \in [0, 1]$, and the uncertainty $\mu(x)$ from x to C is a random number with a stable distribution trend, then the relationship can be expressed by the following relation:

$$\mu(x) : U \to [0, 1] \forall x \in U \tag{1}$$

The distribution of x on the domain U then becomes a cloud model. The quantitative value x is called a cloud droplet, which is used to represent the randomness of the quantitative concept. $\mu(x)$ is used to represent the degree to which the quantitative concept x belongs to the qualitative concept C,and it is called the affiliation function.

The cloud model can not only use the affiliation function $\mu(x)$ to describe the fuzziness of the concept, but also describe the randomness of the affiliation function $\mu(x)$ and the randomness of the cloud droplets. The range of the affiliation degree is from 0 to 1, and the mapping from x to U is one-to-many, indicating that the affiliation degree is a probability distribution rather than a fixed value, resulting in an ambiguous boundary of cloud, which is not a clear curve. A cloud image is composed of multiple cloud droplets, and each cloud droplet reflects the transformation between quantitative data and qualitative data. It is meaningless to analyze the affiliation degree of a certain point separately, and the entirety of each cloud model can reflect the characteristics of qualitative concepts. When the affiliation function satisfies the following formula, the distribution of random variables composed of all cloud droplets is called the normal cloud model. The normal cloud model is the most common cloud model.

$$\mu(x) = \exp\left\{-\frac{(x-Ex)^2}{2y^2}\right\} \tag{2}$$

The cloud generator is a function that establishes the relationship between qualitative and quantitative data, including forward generators, reverse generators, and index approximation methods. This paper uses a reverse generator to estimate the parameters. The statistical method is used to estimate the parameters of the data samples to obtain the digital characteristic parameters of the connotation. In the process of reverse cloud transformation there will inevitably be errors. Excessive prediction faults will make it difficult to achieve two-way transformation between qualitative and quantitative data. The traditional reverse cloud algorithm based on the first-order absolute central moment and the reverse cloud algorithm based on the fourth-order absolute central moment cannot guarantee the following equality. The two algorithms will cause major errors.

$$S^2 - En^2 > 0 \tag{3}$$

$$S^2 = \frac{1}{N-1}\sum_{i=1}^{N}(x_i - \overline{X})^2 \tag{4}$$

$$\overline{X} = \frac{1}{N}\sum_{i=1}^{N} x_i \tag{5}$$

$$En = \sqrt[4]{\frac{9(S^2)^2 - \mu_4}{6}} \tag{6}$$

$$\mu_4 = \frac{1}{N-1}\sum_{i=1}^{N}(x_i - \overline{X})^4 \tag{7}$$

where S^2 is the sample variance, N is the number of samples, x_i is the sample variable, $\overline{X}$ is the average value of the samples, and μ_4 is the fourth-order central moment.

The reverse cloud algorithm based on the first- and fourth-order absolute central moments directly obtains the digital characteristic parameters of the cloud model through the moment estimation of different orders, that is, the single-step estimation, ignoring the characteristics of the cloud droplets being generated by two random processes.

Multiple backward cloud transformation based on sampling replacement (MBCT-SR) was used in this study. MBCT-SR is a multi-step cloud transformation process [30], and through random sampling grouping, E_x and H_e are generated in different subset intervals, which increases the stability [31]. The algorithm for calculating hyperentropy and cloud entropy used in this work can ensure that the estimation of hyperentropy will not appear as an imaginary number and has strong stability [32].

The expectation E_x is the central value of the cloud droplets in the domain space, that is, the average output of the wind–photovoltaic–hydropower complementary power generation system.

$$E_x = \overline{X} = \frac{1}{N}\sum_{i=1}^{n} x_i \tag{8}$$

The entropy E_n is the value range of cloud droplets in the domain space, which reflects the uncertainty information in the cloud model and represents the fluctuation range of output in the complementary system.

$$Y_i^2 = \frac{1}{n-1}\sum_{j=1}^{n} (x_{ij} - \overline{x}_i)^2 \tag{9}$$

$$E_n{}^2 = \frac{1}{2}\sqrt{4(EY^2)^2 - 2Y^2} \tag{10}$$

where Y_i^2 is the variance of random samples by MBCT-SR, n is the number of elements contained in each random sample by MBCT-SR, and x_{ij} is the random samples of MBCT-SR.

The hyper entropy H_e is the uncertainty of the cloud entropy in the domain space, reflecting the randomness of the dispersion and membership degrees of the cloud droplets, and it also describes the concentration degree of the output in the fluctuation range in the complementary system. The greater the hyperentropy, the greater the degree of dispersion of the cloud, the greater the randomness of the membership degree, and the greater the thickness of the cloud.

$$H_e{}^2 = EY^2 - E_n{}^2 \tag{11}$$

Through the above process, a certain input sample is transformed into three eigenvalue forms of the cloud model, and the output quantitative distribution characteristics in each input variable interval are obtained.

An example is displayed for clarity. A cloud model with the parameters $E_x = 4$, $E_n = 1$, and $H_e = 0.1$ is shown in Figure 1. The cloud model uses the distribution of cloud drops to reflect the robustness and fuzziness of the qualitative concept.

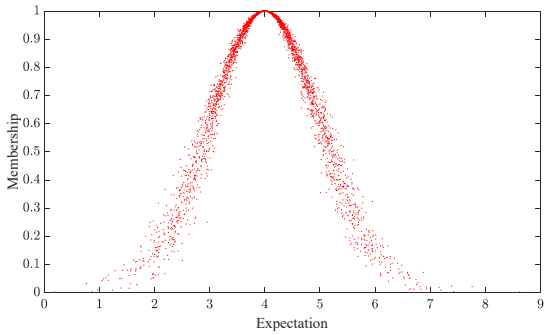

Figure 1. The cloud model concept.

2.2. Output Cloud Similarity

Cloud models can not only provide uncertainty representation in data mining but also provide qualitative analysis methods; this is more in line with human cognition for mining results. In general, quantitative data can be transformed into qualitative data through a cloud model, and data mining tasks based on qualitative concepts require similarity measurements.

According to the output cloud model of wind power, photovoltaic power, and hydropower, the similarity between two output clouds is calculated to reflect and evaluate the degree of correlation between each power generation system, which provides a basis for extracting the complementarity and differences of the wind–photovoltaic, wind–hydropower, and hydropower–photovoltaic power generation systems.

Assuming that the Euclidean distance between the output cloud a and output cloud b is $d_{a,b}$, the calculation formula is as follows [33].

$$d_{a,b} = 1000/\sqrt{(E_{xa} - E_{xb})^2 + (E_{na} - E_{nb})^2 + (H_{xa} - H_{xb})^2} \quad (12)$$

2.3. Correlation Degree Based on the Copula Function

The copula can reflect the multivariate joint probability distribution with marginal distribution [34]. Compared with other simple correlation models, such as the regression model, the copula function can better capture the tail relationship. Therefore, copula functions are generally used to build correlation models for hybrid systems [35]. The copula density can be expressed as

$$U(x_1, x_2, \cdots, x_a) = C(F_1(x_1), F_2(x_2), \cdots F_n(x_a)) \quad (13)$$

where $U(x_a)$ is the joint distribution of variables x_a, and F_a is the marginal distribution of x_a.

If $F(x)$ is a continuous function, the joint probability function can be calculated with (12).

$$u(x_1, x_2, \cdots, x_a) = C(F_1(x_1), F_2(x_2), \cdots F_a(x_a)) \prod_{i=1}^{a} f_a(x_a) \quad (14)$$

where $f(x_a)$ is the marginal density function.

The Kendall coefficient and Spearman rank correlation coefficient were selected as the correlation coefficient methods. The two evaluation indicators were calculated based on a suitable copula function [36].

The Kendall coefficient ρ_τ is calculated as

$$\rho_\tau = P[(A_1 - A_2)(B_1 - B_2) > 0] - P[(A_1 - A_2)(B_1 - B_2) < 0] \quad (15)$$

where $P(\cdot)$ is the probability operation. A_i and B_i are independent variables.

The Spearman rank correlation coefficient ρ_s is calculated as

$$\rho_s = 3\{P[(A_1 - A_2)(B_1 - B_3) > 0] - [(A_1 - A_2)(B_1 - B_3) < 0]\} \quad (16)$$

The copula functions are divided into the elliptic family and the Archimedes family. The elliptic copula contains a Gaussian copula and a t-copula. Compared with the Archimedes copula family, the elliptic family copula can show high-dimensional correlation characteristics. Therefore, this paper selects the Gaussian copula and t-copula to construct the three-dimensional copula function.

The probability distribution function of the Gaussian copula is expressed as

$$C(u_1, u_2, u_3) = \Phi\left(\Phi^{-1}(u_1), \Phi^{-1}(u_2), \Phi^{-1}(u_3)\right) \quad (17)$$

where Φ^{-1} is the inverse function of the standard normal distribution function.

The probability distribution function of the t-copula is expressed as

$$C(u_1, u_2, u_3; \rho, v) = T_{\sum v}(T_v^{-1}(u_1), T_v^{-1}(u_2), T_v^{-1}(u_3)) \quad (18)$$

T_v^{-1} is the inverse function of the unary t distribution function, the degree of freedom of which is v.

The root mean square error ($RMSE$), Akaike information criterion (AIC), and Bayesian information criterion (BIC) were selected to judge the fitness of the model.

$$RMSE = \sqrt{\sum_{i=1}^{n} (E_{pi} - E_i)^2} \quad (19)$$

$$AIC = N\log(\sum_{i=1}^{n}(E_{pi} - E_i)^2) + 2k \tag{20}$$

$$BIC = k\ln(N) + N\log(\sum_{i=1}^{n}(E_{pi} - E_i)^2) \tag{21}$$

where E_{pi} is the predicted value of the copula function, E_i is the real value of the copula function, and k is the number of copula function parameters.

3. Results and Discussion

3.1. Basic Data

This paper takes a wind–photovoltaic–hydropower complementary power generation system in Qinghai, China as an example for analysis. Qinghai Province is located in the northeast of China, and the quantity of wind, photovoltaic, and hydropower is abundant [37]. The rich energy storage volume and vast Gobi desert conditions are appropriate for the development of a hybrid system [38]. The wind–photovoltaic–hydropower hybrid system in the study area was a typical complementary structure, and it clearly reflects the power cases. The actual data of the power generation system from 00:00 on 13 November 2022 to 23:00 on 13 November 2023 were selected to form the data sample library, and the sampling interval was 1 h. The output of the hybrid system in the typical year is shown in Figure 2. In this multi-energy complementary system, due to the proximity to the Yellow River, hydropower resources are abundant, and hydropower output is much larger than wind power and photovoltaic output. In addition, the installed capacity of photovoltaics in this area is small, and the wind power output is greater than the photoelectric output. The wind and photovoltaic output experienced great uncertainty and variability during the analysis. The power distribution of wind is more disperse compared to the photovoltaic output. Compared with renewable energy, the output of hydropower is steadier.

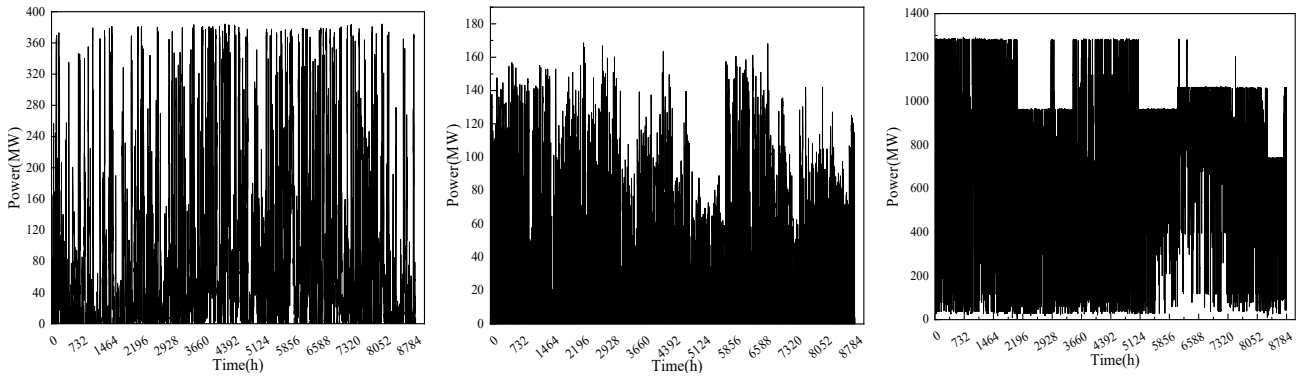

Figure 2. (**a**) Original output of wind in the study area. (**b**) Original output of photovoltaic power in the study area. (**c**) Original output of hydropower in the study area.

Violin plots are used to show the distribution and probability density of multiple sets of continuous data. The size of the box depends on the quartile distance and black area of the data. The large box indicates that the data distribution is discrete and fluctuates greatly, while the small box indicates that the data are concentrated. The distribution of the violin plot in Figure 3 shows that the wind power output is larger in April, May, July, and August, and the degree of dispersion is also larger. The output in September, October, November, and December is more concentrated. The output of photovoltaic power is the largest in July, and the output is significantly larger than that of the other months. The output of photovoltaic power is larger in spring and summer, and the output is more concentrated in autumn and winter. The hydropower output is larger and more concentrated in July and

August, and the output is the most dispersed in December. The output is larger in summer and smaller in winter.

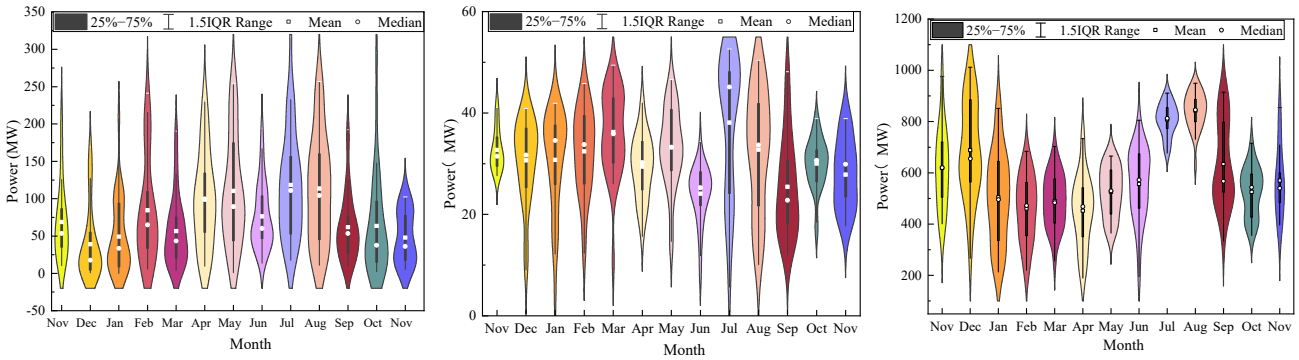

(**a**) (**b**) (**c**)

Figure 3. (**a**) Output characteristics of wind. (**b**) Output characteristics of photovoltaic power. (**c**) Output characteristics of hydropower.

The distribution of the complementary system in each output interval was analyzed using the string diagram in Figure 4, and the normalized output was divided into five intervals: lowest, lower, medium, higher, and highest output intervals. The wind power output was concentrated in the [0,0.2] output interval, and the cumulative normalized output reached 2.75. The output probability interval in summer was larger, and the output probability interval in autumn was smaller. The photovoltaic output was also concentrated in the [0,0.2] interval, and the cumulative normalized output reached 2.65. For the photovoltaic output, the probability interval of [0.8–1] was the smallest, and the photovoltaic output was largest in summer. The distribution of hydropower output in each interval is relatively uniform, and the probability was larger in the output interval of [0.6–0.8] and greater in summer.

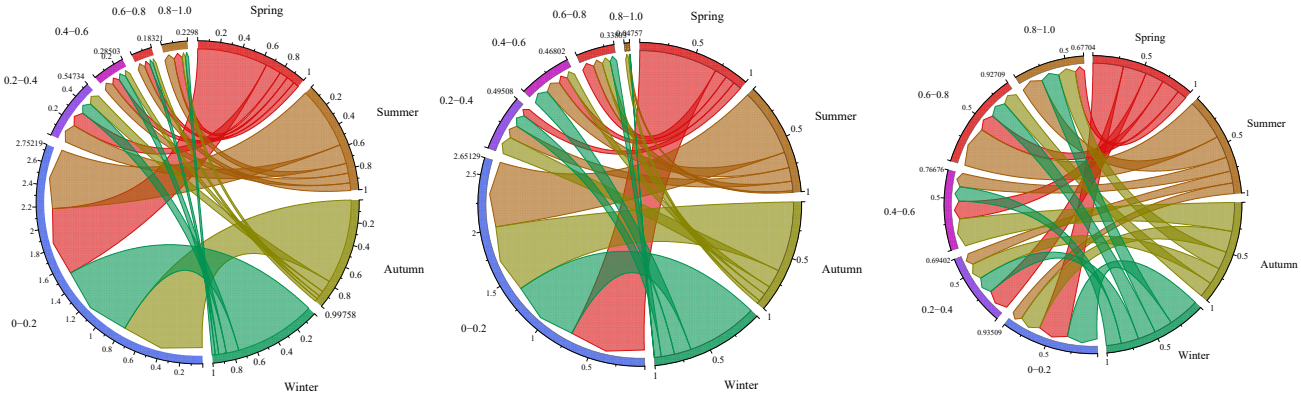

(**a**) (**b**) (**c**)

Figure 4. (**a**) Probability distribution of wind. (**b**) Probability distribution of photovoltaic power. (**c**) Probability distribution of hydropower.

3.2. Output Cloud Model Analysis

The wind power output, photovoltaic output, and hydropower output were divided into intervals of 35 MW wind power output, 17 MW photovoltaic output, and 129 MW hydropower output, and the outputs of different input variable intervals were counted. The results are shown in Figures 5–7.

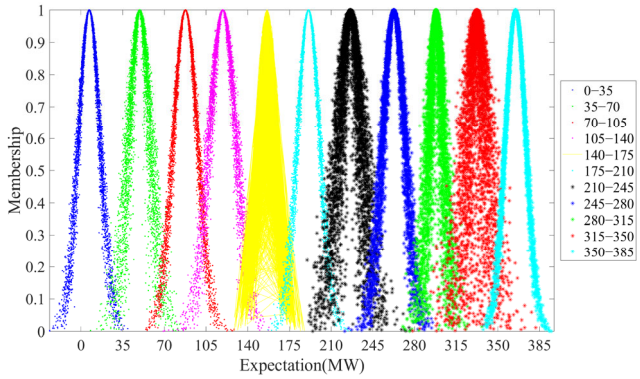

Figure 5. Output cloud of the different wind power output intervals.

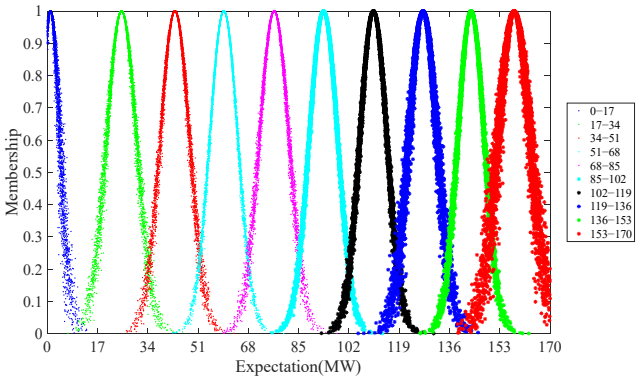

Figure 6. Output cloud of the different photovoltaic power output intervals.

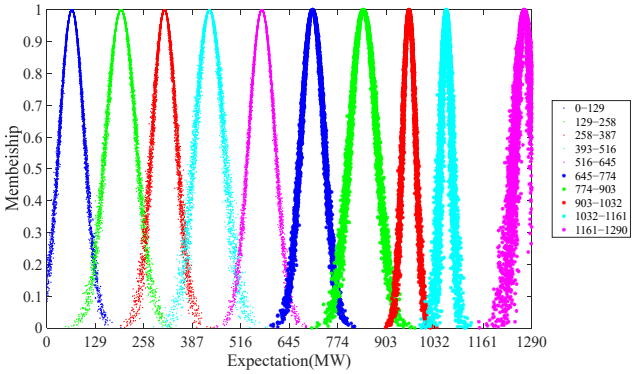

Figure 7. Output cloud of the different hydropower output intervals.

By constructing the output cloud model of three power sources, the output distribution, fluctuation, and concentration can be seen. In the wind power output distribution between 0 and 385 MW, the entropy in the [105,140] output interval is 11.1638, indicating that the output fluctuation in this interval is large. The entropy in the [280,315] output interval is 5.8725, and the output varies smoothly. The hyperentropy in the [315,350] output interval is 4.735, indicating that the output dispersion in this interval is greater. The hyperentropy in the [350,385] output interval is 0.6644, and the output concentrates in this interval. Overall, the hyperentropy of wind power in each output interval is larger, the dispersion degree of fluctuation is larger, and it has strong uncertainty.

The photovoltaic output is distributed between 0 and 170 MW, with the lowest expected output. The fluctuation range of the output in each output interval does not differ by much. The entropy in the [153–170] interval is 5.4985, and this is the maximum of the photovoltaic power entropy. The output dispersion in the [153,170] interval is large. The

output fluctuation of photovoltaic output in each interval is relatively average, and the overall photovoltaic output is relatively stable.

The hydropower output is distributed between 0 and 1290 MW. The entropy in the [1032,1161] output interval is only 14.7385, and the fluctuation degree is the smallest. The entropy of hydropower is the greatest for the hybrid system, indicating that the fluctuation in hydropower is much larger than wind and photovoltaic power in the output interval. The hyperentropy in the [903,1032] output interval is 1.8326, and the output is the most concentrated.

Compared with the output scatter diagram, which can only qualitatively reflect the output trend and fluctuation of the power generation system, the output cloud model quantitatively reflects the output characteristics of each power generation system from qualitative evaluation to quantitative evaluation. It also more intuitively and comprehensively reflects the fluctuation and dispersion degree of each power generation system.

3.3. Cloud Model Similarity

According to the calculation method of cloud similarity, the monthly average outputs of wind power, photovoltaic power, and hydropower were used to calculate the cloud similarity of wind power–photovoltaic power, wind power–hydropower, and photovoltaic power–hydropower generation systems in each month. The results are shown in Table 1.

Table 1. Cloud similarity value of every month.

Complementary System	Wind–Photovoltaic	Wind–Hydropower	Photovoltaic–Hydropower
January	29.995	1.910	1.881
February	17.668	2.302	2.099
March	29.761	1.957	1.927
April	14.417	2.439	2.111
May	12.710	2.018	1.780
June	18.465	1.925	1.743
July	12.302	1.377	1.242
August	11.891	1.269	1.160
September	27.297	1.596	1.513
October	26.120	1.897	1.809
November	23.981	1.665	1.635
December	23.182	1.367	1.379

The wind–photovoltaic complementary system has the highest similarity in January, reaching 29.995, and the highest complementarity in July, with a similarity of 11.891. The wind–hydropower complementary system has the highest similarity in April, reaching 2.439, and the highest complementarity in August, with a similarity of 1.269. The photovoltaic–hydropower complementary system has the highest similarity in April, reaching 2.111, and the highest complementarity in August, with a similarity of 1.160. It can be seen from the above table that the similarity between wind power and photovoltaic power is the highest of the three hybrid systems. In summer, the difference between wind and photovoltaic power output is larger. The similarity between wind power and hydropower, photovoltaic power, and hydropower is the highest in spring, and the difference in summer is the largest. In the summer, hydropower can effectively adjust the wind and photovoltaic power output. The output similarity cloud reflects the difference and complementarity between the output clouds.

3.4. Correlation Analysis of Hybrid Systems

Furthermore, to analyze the correlation of the hybrid systems, the Kendall correlation coefficient and Spearman rank coefficient were used in this study to judge the three-dimensional correlation coefficient. The goodness-of-fit test results are shown in Table 2.

The RMSE, AIC, and BIC of the Gaussian copula are all smaller than the t-copula. Therefore, the Gaussian copula was selected to fit the model.

Table 2. Three-dimensional copula function of the goodness-of-fit test.

Copula Function	RMSE	AIC	BIC
Gaussian copula	0.0138	−7520	−7759
t-copula	0.0190	−6965	−7741

Through the comparison of the two correlation coefficients in Figure 8, it was found that the correlation between photoelectricity and hydropower is the largest, with the Kendall correlation coefficient and Spearman rank coefficient being −0.2215 and −0.3272, respectively. This indicates that hydropower has a high correlation with photoelectricity. The period of large hydropower output is generally when the summer rainfall is large, and at this time, the photovoltaic panel can rarely receive sunlight and generate electricity; therefore, there is a significant negative correlation between the two. The correlation between wind power and hydropower is the smallest, with the Kendall correlation coefficient and Spearman rank coefficient being 0.04388 and 0.06578, respectively. The two correlation coefficients between wind and hydropower are positive, indicating that hydropower and wind power have similar output distributions. Based on the real-world scenario of Qinghai Province, hydropower plays an important role in regulating the output of renewable energy in the complementary system. The correlation coefficient between wind power and photovoltaic power is involved in the correlation coefficient between the other two systems, indicating that there is a certain negative correlation between wind power and photovoltaic power. In the period of large wind power output, photovoltaic output is often small, and this complementary relationship can be used to adjust the daily output of the system.

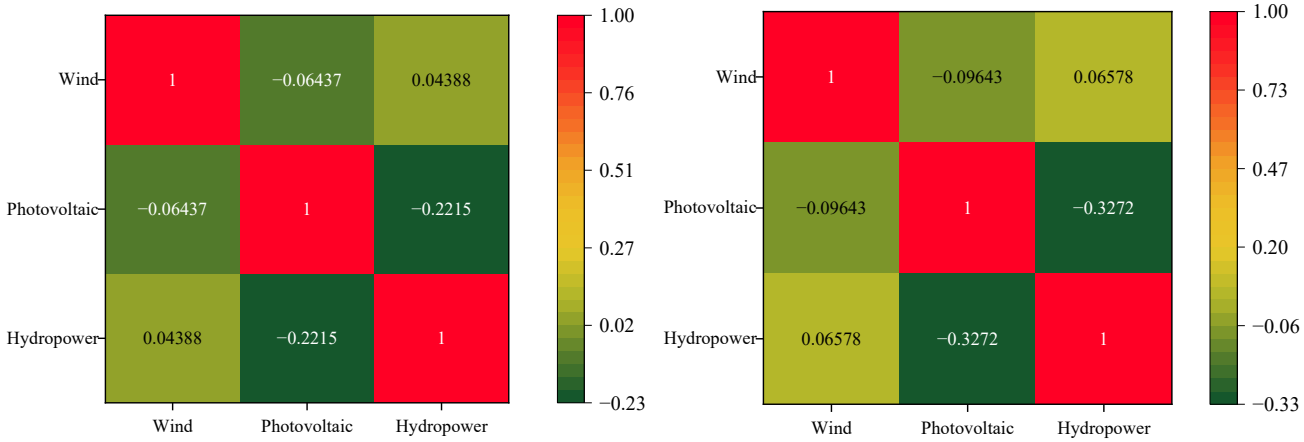

Figure 8. (**a**) Kendall correlation coefficient of the Gaussian copula. (**b**) Spearman rank coefficient of the Gaussian copula.

4. Conclusions

In the current energy context, future power systems are trending toward the construction of a high proportion of wind–photovoltaic–hydro complementary systems. Due to the fluctuation and dispersion of wind power, PV power, and hydropower, it is difficult to accurately quantify the output characteristics of the power generation system. Therefore, a cloud model was constructed in this study to characterize the volatility and dispersion of the complementary system. The MBCT-SR method was proposed to calculate the improved entropy and hyperentropy to quantitatively analyze the fluctuation range and dispersion degree. The similarity index of the output cloud and Kendall and Spearman coefficients of

the Gaussian copula was proposed to evaluate the temporal and spatial characteristics of wind–photovoltaic–hydropower hybrid power output.

(1) The cloud model can be extended from qualitative to quantitative evaluation, which can more accurately reflect the output characteristics. Correlation analysis can characterize the similarity of complementary power generation systems.
(2) The hyperentropy of the hydropower system is larger than others, meaning the output of hydropower is more concentrated in the interval between 1161 and 1290, and thus the degree of dispersion in the output interval is greater. The wind and photovoltaic outputs have better similarity in January; the index of similarity is 29.995.
(3) Due to the RMSE, AIC, and BIC, the Gaussian copula is more suitable for describing hybrid systems. The Kendall correlation and Spearman rank correlations of the Gaussian copula were -0.2215 and -0.3272, respectively. The results suggest that the correlation between hydropower and photovoltaic power is better.

In practical applications, the cloud model for hybrid power generation systems can provide a demand reference for peak regulation. The similarity index of the cloud model and Gaussian copula function will promote analysis of the interaction of each subsystem in the hybrid power system.

Author Contributions: Conceptualization, H.M. and F.X.; methodology, H.M. and P.H.; software, C.L.; investigation, C.L. and L.Y.; resources, L.Y.; writing—original draft preparation, H.M. and P.H.; writing—review and editing, H.M. and F.X.; supervision, F.X. All authors have read and agreed to the published version of the manuscript.

Funding: The work was supported by the Science and Technology project of Qinghai Province (2023-GX-158).

Data Availability Statement: The data are available in this paper.

Acknowledgments: The authors thank the reviewers whose comments improved the quality of this paper.

Conflicts of Interest: Authors Chunlai Li and Libin Yang were employed by the State Grid Qinghai Electric Power Company. The remaining authors declare that the research was conducted in the absence of any commercial or financial relationships that could be construed as a potential conflict of interest.

Nomenclature

MBCT-SR	Multiple backward cloud transformation based on sampling with replacement	Y^2	Variance of random samples by MBCT-SR
RMSE	Root mean square error	d	Euclidean distance between the output clouds
AIC	Akaike information criterion	$U(\cdot)$	Joint distribution of variables
BIC	Bayesian information criterion	F_a	Marginal distribution of variables
Parameters		$u(\cdot)$	Joint probability function of variables
E_x	Expectation value	f_a	Marginal density function.
E_n	Entropy	C	Set of marginal distribution function
H_e	Hyperentropy	ρ_τ	Kendall coefficient
U	Domain of discourse	ρ_s	Spearman rank correlation coefficient
C	Random qualitative concept	AB	Independent random vectors
$\mu(x)$	Affiliation function	Φ^{-1}	Inverse function of the standard normal distribution function
S^2	Variance of samples	T_v^{-1}	Inverse function of the unary t distribution function
N	Number of samples	v	Degree of freedom
x_i	Sample variable	E_{pi}	Predicted value of copula function
$\overline{X}$	Average value of samples	E_i	Real value of copula function
μ_4	Fourth-order central moment	k	Number of copula function parameters

References

1. Shayan, M.E.; Najafi, G.; Ghobadian, B.; Gorjian, S.; Mazlan, M.; Samami, M.; Shabanzadeh, A. Flexible Photovoltaic System on Non-Conventional Surfaces: A Techno-Economic Analysis. *Sustainability* **2022**, *14*, 3566. [CrossRef]
2. Zhu, F.; Zhong, P.; Xu, B.; Liu, W.; Wang, W.; Sun, Y.; Chen, J.; Li, J. Short-Term Stochastic Optimization of a Hydro-Wind-Photovoltaic Hybrid System under Multiple Uncertainties. *Energy Convers. Manag.* **2020**, *214*, 112902. [CrossRef]
3. Huang, K.; Liu, P.; Ming, B.; Kim, J.S.; Gong, Y. Economic Operation of a Wind-Solar-Hydro Complementary System Considering Risks of Output Shortage, Power Curtailment and Spilled Water. *Appl. Energy* **2021**, *290*, 116805. [CrossRef]
4. Chen, Y.; Wang, Y.; Kirschen, D.; Zhang, B. Model-Free Renewable Scenario Generation Using Generative Adversarial Networks. *IEEE Trans. Power Syst.* **2018**, *33*, 3265–3275. [CrossRef]
5. Zhang, Y.; Lian, J.; Ma, C.; Yang, Y.; Pang, X.; Wang, L. Optimal Sizing of the Grid-Connected Hybrid System Integrating Hydropower, Photovoltaic, and Wind Considering Cascade Reservoir Connection and Photovoltaic-Wind Complementarity. *J. Clean. Prod.* **2020**, *274*, 123100. [CrossRef]
6. Shayan, M.E.; Najafi, G.; Ghobadian, B.; Gorjian, S.; Mazlan, M. A Novel Approach of Synchronization of the Sustainable Grid with an Intelligent Local Hybrid Renewable Energy Control. *Int. J. Energy Environ. Eng.* **2023**, *14*, 35–46. [CrossRef]
7. AN, Y.; Zhao, Z.; Wang, S.; Huang, Q.; Xie, X. Coordinative Optimization of Hydro-Photovoltaic-Wind-Battery Complementary Power Stations. *CSEE J. Power Energy Syst.* **2020**, *6*, 410–418. [CrossRef]
8. Tang, Y.; Fang, G.; Tan, Q.; Wen, X.; Lei, X.; Ding, Z. Optimizing the Sizes of Wind and Photovoltaic Power Plants Integrated into a Hydropower Station Based on Power Output Complementarity. *Energy Convers. Manag.* **2020**, *206*, 112465. [CrossRef]
9. Xu, B.; Zhu, F.; Zhong, P.; Chen, J.; Liu, W.; Ma, Y.; Guo, L. Identifying Long-Term Effects of Using Hydropower to Complement Wind Power Uncertainty through Stochastic Programming. *Appl. Energy* **2019**, *253*, 113535. [CrossRef]
10. Wang, X.; Chang, J.; Meng, X.; Wang, Y. Short-Term Hydro-Thermal-Wind-Photovoltaic Complementary Operation of Interconnected Power Systems. *Appl. Energy* **2018**, *229*, 945–962. [CrossRef]
11. Hu, X.; Min, H.; Dai, S.; Cai, Z.; Yang, X.; Ding, Q.; Yang, Z.; Xiao, F. Research on Maintenance Strategies for Different Transmission Sections to Improve the Consumption Rate Based on a Renewable Energy Production Simulation. *Energies* **2022**, *15*, 9262. [CrossRef]
12. Wang, F.; Xie, Y.; Xu, J. Reliable-Economical Equilibrium Based Short-Term Scheduling towards Hybrid Hydro-Photovoltaic Generation Systems: Case Study from China. *Appl. Energy* **2019**, *253*, 113559. [CrossRef]
13. Li, Q.; Zhang, Y.; Liu, W.; Li, Z.; Chen, J.; Hu, J.; Liang, S. Analysis of Output Coupling Characteristics among Multiple Photovoltaic Power Stations Based on Correlation Coefficient. *Energy Rep.* **2022**, *8*, 908–915. [CrossRef]
14. Zhao, S.; Jin, T.; Li, Z.; Liu, J.; Li, Y. Wind Power Scenario Generation for Multiple Wind Farms Considering Temporal and Spatial Correlations. *Dianwang Jishu Power Syst. Technol.* **2019**, *43*, 3997–4004. [CrossRef]
15. Chen, J.J.; Zhuang, Y.B.; Li, Y.Z.; Wang, P.; Zhao, Y.L.; Zhang, C.S. Risk-Aware Short Term Hydro-Wind-Thermal Scheduling Using a Probability Interval Optimization Model. *Appl. Energy* **2017**, *189*, 534–554. [CrossRef]
16. Tan, Q.; Wen, X.; Sun, Y.; Lei, X.; Wang, Z.; Qin, G. Evaluation of the Risk and Benefit of the Complementary Operation of the Large Wind-Photovoltaic-Hydropower System Considering Forecast Uncertainty. *Appl. Energy* **2021**, *285*, 116442. [CrossRef]
17. He, Y.; Wang, M. Applicability Evaluation of China' s Retail Electricity Price Package Combining Data Envelopment Analysis and a Cloud Model. *Energies* **2020**, *13*, 6. [CrossRef]
18. Liu, T.; Min, H.; Li, C.; Zhou, W.; Xiao, F. MBCT-SR Coupled Cloud Model for Wind-Photovoltaic-Hydro Hybrid Power Generation System. In Proceedings of the 2022 6th International Conference on Power and Energy Engineering (ICPEE 2022), Shanghai, China, 25–27 November 2022; pp. 7–11.
19. Zhu, Y.; Li, J.; Lan, X.; Lu, S.; Yu, J. Research on Evaluation Method of Digital Project Cloud Model Considering Weight Sensitivity. *Energies* **2022**, *15*, 5738. [CrossRef]
20. Chen, S.; Guo, X.; Han, S.; Xiao, J.; Wu, N. A Novel Stochastic Cloud Model for Statistical Characterization of Wind Turbine Output. *IEEE Access* **2021**, *9*, 7439–7446. [CrossRef]
21. Wang, Q.; Gong, R.; Qin, L.; Feng, Z. Control Strategy for Buck DC/DC Converter Based on Two-Dimensional Hybrid Cloud Model. *J. Electr. Eng. Technol.* **2016**, *11*, 1684–1692. [CrossRef]
22. Lei, J.; Gong, Q. Comprehensive Prediction Method for Failure Rate of Transmission Line Based on Multi-Dimensional Cloud Model. *IET Gener. Transm. Distrib. Res.* **2019**, *13*, 1672–1678. [CrossRef]
23. Dong, J.; Wang, D.; Liu, D.; Ainiwaer, P.; Nie, L. Operation Health Assessment of Power Market Based on Improved Matter-Element Extension Cloud Model. *Sustainability* **2019**, *11*, 5470. [CrossRef]
24. Wang, M.; Li, C.; Wang, X.; Piao, Z.; Yang, Y.; Dai, W.; Zhang, Q. Research on Comprehensive Evaluation and Early Warning of Transmission Lines' Operation Status Based on Dynamic Cloud Computing. *Sensors* **2023**, *23*, 1469. [CrossRef]
25. Goh, H.H.; Peng, G.; Zhang, D.; Dai, W.; Kurniawan, T.A.; Goh, K.C.; Cham, C.L. A New Wind Speed Scenario Generation Method Based on Principal Component and R-Vine Copula Theories. *Energies* **2022**, *15*, 2698. [CrossRef]
26. Zhang, X.; Zhu, H.; Li, B.; Wu, R.; Jiang, J. Power Transformer Diagnosis Based on Dissolved Gases Analysis and Copula Function. *Energies* **2022**, *15*, 4192. [CrossRef]
27. Shan, B.; Guo, S.; Wang, Y.; Li, H.; Guo, P. Vine Copula and Cloud Model-Based Programming Approach for Agricultural Water Allocation under Uncertainty. *Stoch. Environ. Res. Risk Assess.* **2021**, *35*, 1895–1915. [CrossRef]

28. Lin, Y.; Ji, T.; Jiang, Y.; Wu, Q.H. Stochastic Economic Dispatch Considering the Dependence of Multiple Wind Farms Using Multivariate Gaussian Kernel Copula. *CSEE J. Power Energy Syst.* **2022**, *8*, 1352–1362. [CrossRef]
29. Dong, X.; Zhang, X.; Zhang, G.; Wang, S. Analysis of Wind Turbine Output Power Characteristic Based on Cloud Model. *J. Mech. Eng.* **2017**, *53*, 198–205. [CrossRef]
30. Liang, X.; Liang, W.; Zhang, L.; Guo, X. Risk Assessment for Long-Distance Gas Pipelines in Coal Mine Gobs Based on Structure Entropy Weight Method and Multi-Step Backward Cloud Transformation Algorithm Based on Sampling with Replacement. *J. Clean. Prod.* **2019**, *227*, 218–228. [CrossRef]
31. Xu, C.; Wang, G. Bidirectional Cognitive Computing Model for Uncertain Concepts. *Cognit. Comput.* **2019**, *11*, 613–629. [CrossRef]
32. Xu, J.; Ding, R.; Li, M.; Dai, T.; Zheng, M.; Yu, T.; Sui, Y. A New Bayesian Network Model for Risk Assessment Based on Cloud Model, Interval Type-2 Fuzzy Sets and Improved D-S Evidence Theory. *Inf. Sci.* **2022**, *618*, 336–355. [CrossRef]
33. Hosseini, F.; Safari, A.; Farrokhifar, M. Cloud Theory-Based Multi-Objective Feeder Recon Fi Guration Problem Considering Wind Power Uncertainty. *Renew. Energy* **2020**, *161*, 1130–1139. [CrossRef]
34. Rajabalizadeh, S. A Practicable Copula-Based Approach for Power Forecasting of Small-Scale Photovoltaic Systems. *IEEE Syst. J.* **2020**, *14*, 4911–4918. [CrossRef]
35. Wang, Y.; Yang, R.; Xu, S.; Tang, Y. Capacity Planning of Distributed Wind Power Based on a Variable-Structure Copula Involving Energy. *Energies* **2020**, *13*, 3602. [CrossRef]
36. Liu, X.; Wang, L.; Cao, Y.; Ma, R.; Wang, Y.; Li, C.; Liu, R. Renewable Scenario Generation Based on the Hybrid Genetic Algorithm with Variable Chromosome Length. *Energies* **2023**, *16*, 3180. [CrossRef]
37. Esmaeili Shayan, M.; Ghasemzadeh, F.; Rouhani, S.H. Energy Storage Concentrates on Solar Air Heaters with Artificial S-Shaped Irregularity on the Absorber Plate. *J. Energy Storage* **2023**, *74*, 109289. [CrossRef]
38. Shayan, M.E.; Najafi, G.; Ghobadian, B.; Gorjian, S.; Mamat, R.; Ghazali, M.F. Multi-Microgrid Optimization and Energy Management under Boost Voltage Converter with Markov Prediction Chain and Dynamic Decision Algorithm. *Renew. Energy* **2022**, *201*, 179–189. [CrossRef]

Disclaimer/Publisher's Note: The statements, opinions and data contained in all publications are solely those of the individual author(s) and contributor(s) and not of MDPI and/or the editor(s). MDPI and/or the editor(s) disclaim responsibility for any injury to people or property resulting from any ideas, methods, instructions or products referred to in the content.